Rare Metal Materials and Engineering
Volume 47, Issue 4, April 2018
Online English edition of the Chinese language journal

Available online at www.sciencedirect.com

Cite this article as: Rare Metal Materials and Engineering, 2018, 47(4): 1113-1118.

ARTICLE

Well-aligned Au/TiO_2 Nanorods Arrays for the Photodegradation of MB by Magnetron Sputtering

Kong Shaoqi[1,2], **Song Xuanmin**[1,2], **Sun Zedong**[1,2], **Zhang Chunwang**[1,2], **Yan Guochao**[1,2]

[1] College of Mining Engineering, Taiyuan University of Technology, Taiyuan 030024, China; [2] Institute of Mining Technology, Taiyuan University of Technology, Taiyuan 030024, China

Abstract: The growth of well-aligned Au/TiO_2 nanorods arrays was performed by magnetron sputtering. The feasibility of preparing Au/TiO_2 nanorods was demonstrated via dc reactive magnetron sputtering at room temperature and heat-treatment at 500 ºC in air for 2 h. The results show that the heat treatment leads to the formation of Au/TiO_2 nanorods with Au nanoparticles embedded in the TiO_2 nanorods of anatase phase. These Au/TiO_2 nanorods show lower photoluminescence emission intensity and higher absorption and intensive response to the visible light, compared with traditional TiO_2 nanofilms fabricated by the traditional method. The Au nanoparticles in the TiO_2 nanorods suppress the charge recombination.

Key words: Au-TiO_2 nanorods; photodegradation; magnetron sputtering; photoluminescence emission intensity

Titanium dioxide (TiO_2) and TiO_2-based materials have been extensively studied, which have important applications in many fields such as heterogeneous catalysis, energy storage, sensor design, electric device design, wastewater purification[1,2]. Recently, much interest has been devoted to the use of TiO_2-based photocatalysts for the degradation of dyes in aqueous solutions[3-8]. It is used not only in solar cells as a photo-catalyst for the production of hydrogen and electric energy but also for photo-assisted degradation of organic molecules.

There is growing interest in developing new advanced materials and designing novel devices with control features on nanometer scales[9,10]. Nanostructured TiO_2-based materials (e.g. nanoparticles[11], nanotubes, nanofibers[12,13] and nanoporous structures[14]) have been receiving significant attention. Nanorod and nanowire have attracted much attention since oriented nanorod or nanowire arrays provide a direct path for electron diffusion, leading to increased electron diffusion rate and higher solar cell performance. Commonly used methods for the synthesis of nanomaterials include sol gel, hydrothermal synthesis, vapor phase transport, electrochemical synthesis, arc discharge, laser ablation and CVD[15-17]. Currently, TiO_2 nanorod arrays have been synthesized by oxidizing titanium with acetone[18], using a hydrothermal method on fluorine-doped tin oxide (FTO) glass[19,20] and by a dc reactive magnetron sputtering technique[21]. However, there is seldom report of Au/TiO_2 nanowires or nanorods synthesized by the sputtering technique, even though the sputtering process has been used to synthesize nano-structures and nanowires of various materials so far.

In the present paper, the synthesis of well-aligned Au/TiO_2 nanorods arrays by magnetron sputtering process is described. Au/TiO_2 nanorods were grown on ITO (indium tin oxide) substrates. In the following sections, details of the experimental procedure, characterization of the samples, and discussion of the results will be presented.

1 Experiment

Au nanofilms on ITO substrates (1 cm × 1 cm) were prepared at room temperature (25 °C) by magnetron sputtering in a multifunctional magnetron sputtering instrument (JGP560B) under the condition of high vacuum, using an Au target (99.9%). Prior to deposition, the ITO substrates were ultrasonically cleaned with acetone, ethyl alcohol, and

---

Received date: April 20, 2017
Foundation item: Youth Science and Technology Research Foundation of Shanxi (20150211)
Corresponding author: Song Xuanmin, Ph. D., Professor, Institute of Mining Technology, Taiyuan University of Technology, Taiyuan 030024, P. R. China, Tel: 0086-351-6014627, E-mail: xminsong@163.com

de-ionized (DI) water for 20 min, and dried at room temperature before being placed into the sputtering chamber. Argon gas was flowed into the sputtering chamber after the pressure of the sputtering chamber reached 8×10^{-4} Pa. Pre-sputtering of 3 min was performed to remove surface residuals. The flow rate of argon gas was 30 cm^3/min and the chamber pressure was 6 Pa during the deposition. The distance between the ITO substrate and the target was 60 mm, and the thickness of Au nanofilms was ~30 nm, which was controlled by the sputtering time.

After the deposition of Au nanofilms, a TiO_2 target was used to deposit TiO_2 films with ~270 nm thickness on the Au films, using a similar approach and similar conditions. The prepared Au-TiO_2 bilayer nanofilms were heat-treated at 500 °C for 2 h at a ramping rate of 2 $^{o}C\cdot min^{-1}$ in a furnace in air.

The surface topology of the prepared Au/TiO_2 nanorods was examined, using a field emission scanning electron microscopy (FESEM) (Tescan MIRA 3 LMH) at 10 kV; a transmission electron microscopy (TEM, JEM2100, JEOL). Before TEM measurement, the Au/TiO_2 nanorods arrays were carefully scraped from the substrate and dispersed in ethanol solution. After ultrasonic dispersion for 5 min, the solution was dipped on a copper screen for TEM observation. The composition of the Au/TiO_2 nanorods was determined using energy dispersive spectroscopy (EDS) (OXFORD X-Max 20). The crystal structures of the Au/TiO_2 nanorods were analyzed with the Cu Kα line on a Rigaku D/max 2500 X-ray diffraction (XRD) with patterns recorded in a range of 20°~80°. Optical absorptions of the Au/TiO_2 nanorods in the wavelength range of 300~800 nm was measured using a UV-vis spectrophotometer (Perkin-Elmer, Lambda 750). The banding energy was determined by X-ray photoelectron spectroscopy (XPS) (Escalab 250).

Photoelectrochemical analysis of the prepared Au/TiO_2 nanorods was conducted in a three-electrode cell, in which the prepared Au/TiO_2 nanorods, a Pt foil, and SCE (saturated calomel electrode) were used as working, counter, and reference electrodes, respectively. The electrolyte was 0.1 mol/L Na_2S aqueous solution purged with N_2 gas for 30 min. A 500 W Xenon lamp (TrustTech, Beijing, China) with a cutoff filter (λ>420 nm) was used as the light source. The photocurrent was recorded by a CHI660D electrochemical workstation.

The photocatalytic activity of the prepared Au/TiO_2 nanorods was evaluated by measuring the degradation behavior of the MB organic compound in an aqueous solution under the irradiation of visible light. The MB aqueous solution (5 $mg\cdot L^{-1}$) of 50 mL was placed in a shallow, round glass vessel with a diameter of 4.5 cm and stirred in the dark at room temperature for 30 min. Three rectangular glass slides of 10 mm×10 mm with the Au/TiO_2 nanorods were placed in the vessel, which was adequate under the experimental conditions without disturbing the visible light entering the glass vessel. The glass vessel was placed in an ice bath to maintain a constant temperature during the characterization of the photocatalytic activity. A 300 W tungsten lamp (Philips Halogen) with a cutoff filter (λ>420 nm) at a distance of 20 cm above the solution was used to irradiate the aqueous MB solutions. The adsorption of MB on the surface of the Au/TiO_2 nanorods led to the decrease of the MB concentration in the aqueous solution and the change of the absorbance of the MB aqueous solutions under the irradiation of visible light. To eliminate the effect of background, the photo-induced reactions were performed after mixing the Au/TiO_2 nanorods with the MB solution in the dark for half an hour to reach a steady state. All the samples for the experiment of photocatalytic activity were calcined at 500 °C.

The photo-induced MB degradation was thus determined from the absorbance of the MB peak at a wavelength of 664 nm, using a UV/vis spectrophotometer (Perkin-Elmer, Lambda 750), from which the MB concentration, c, was estimated as,

$$c=A_0/A \quad (1)$$

where A_0 is the absorbance of MB at the beginning of the irradiation of visible light, and A is the absorbance of MB at time t. The rate constant, k, is calculated as,

$$\ln(c_0/c)=\ln(A/A_0)=kt \quad (2)$$

where c_0 is the concentration of the MB solution without visible light irradiation.

2 Results and Discussion

2.1 SEM and EDS analysis of Au/TiO_2 nanorods

Fig.1a and 1b show top-view SEM micrographs of the prepared Au/TiO_2 nanorods over a large area. The surface is rough, and there are irregular tips (islands) on top of the Au/TiO_2 nanorods. The SEM image of the cross-section of the Au/TiO_2 nanorods (Fig.1c) shows a cleavage surface. There is no bilayer structure left after the heat treatment. The bilayer structure grew into a single layer structure due to the migration of Au atoms into the TiO_2 film during the calcination[22]. Fig.1d shows the EDS spectrum of the Au/TiO_2 nanorods, confirming the presence of Au, Ti, and O.

From the SEM image, the thickness of the layer consisting of the Au/TiO_2 nanorods is found to be ~320 nm, which is slightly larger than 300 nm (30 nm+270 nm) of the summation of the thicknesses of gold film and TiO_2 film. The change in the resultant thickness of the film is likely due to the formation of gold nanoparticles in TiO_2 nanorods, which introduces local expansion. It is expected that the rough top surface of the aligned Au/TiO_2 nanorods will provide a large surface area for dye loading, and the Au/TiO_2 nanorods on the ITO substrates can reduce the loss of electrons during the transfer of photo-generated electrons along the nanorods[23].

2.2 TEM, HETEM and SAED analysis of Au/TiO_2 nanorods

The TEM observation was performed on the Au/TiO_2 nanorod arrays, which were carefully scraped from an ITO

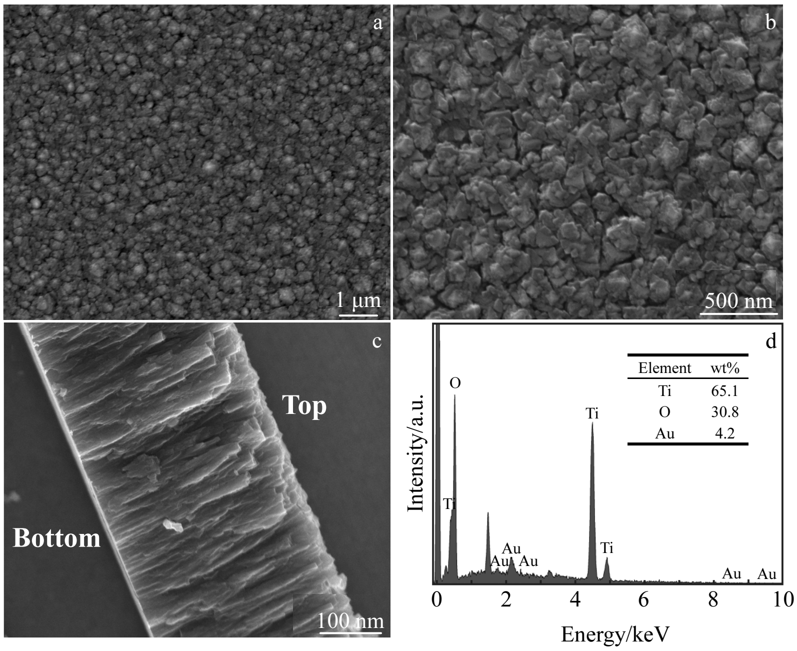

Fig.1 SEM images (a~c) and EDS spectrum (d) of the prepared Au/TiO_2 nanorod arrays

substrate and dispersed in an ethanol solution. Fig.2a and 2b are the low-resolution TEM images of aligned Au/TiO_2 nanorods. It is evident that Au/TiO_2 nanorods with average diameter of about 100 nm are formed. To further illuminate the detailed microstructures, the corresponding HRTEM image of Fig.2b is shown in Fig.2c. There are well-resolved {001} lattice fringes (*d*=0.35 nm) of anatase TiO_2, and {111} lattice fringes (*d*=0.24 nm) of Au. The lattice fringes observed suggest that the resultant Au/TiO_2 nanorods have good crystallinity. The selected area electron diffraction (SAED) pattern (Fig.2d), which was taken in the fringe of Fig.2b, confirms the crystallinity of the Au/TiO_2 nanorods. All of these results suggest that the heat-treatment of the bilayer Au/TiO_2 structure on ITO substrate at 500 ºC in air for 2 h leads to the formation of Au/TiO_2 nanorods with good crystallinity and the embedment of Au nanoparticles in the TiO_2 nanorods.

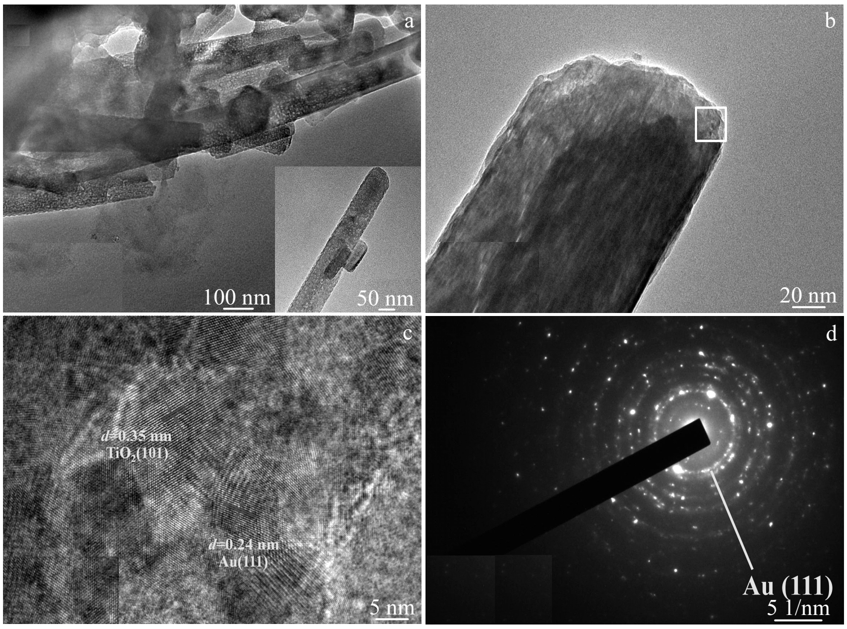

Fig.2 TEM images (a, b), HRTEM image (c) and SAED pattern (d) of the prepared Au/TiO_2 nanorod arrays

2.3 XRS analysis of Au/ TiO_2 nanorods

As shown in Fig.3a, for the traditional TiO_2 nanofilms, all the diffraction peaks can be indexed as the typical anatase phase of TiO_2 in agreement with the values in the standard card. The diffraction peaks at 2θ values of 25.3°, 37.9°, and 48.2° are attributed to (101), (004) and (200) planes of crystalline anatase TiO_2 (JCPDS 77-0443), respectively. The XRD patterns of Au/TiO_2 nanorods loading Au show that the peak at 2θ=38.2° and 77.5° can be indexed to the (111) and (311) face of the cubic phase of Au[24], respectively, demonstrating the existence of Au. From the XPS analysis in Fig.3b, Au and Ti are presented in the Au/TiO_2 nanorods by magnetron sputtering. Fig.3c shows the Au 4f fine XPS spectra of the Au/TiO_2 nanorods. The binding energies for Au $4f_{7/2}$ and Au $4f_{5/2}$ are found to be ca. 83.11 and 86.81 eV. This result indicates that Au is present at zero-valence state (Au^0) and there is no gold oxide[25,26]. Fig.3d compares the two samples in Ti 2p. The two peaks at ca. 458.5 and 464.2 eV correspond to the binding energies of Ti $2p_{3/2}$ and Ti $2p_{1/2}$ levels, respectively, which reveals the presence of the Ti (IV) state.

2.4 UV-vis diffuse reflection spectra

From UV-vis diffuse reflection spectra shown in Fig.4a, it is obvious that the Au/TiO_2 nanorods show enhanced absorption in both the UV and visible light regions compared with traditional TiO_2 nanofilms prepared by magnetron sputtering. The absorption edge of aligned TiO_2 nanorods undergoes an obvious red shift, yielding a band gap (E_g) of 3.08 eV (the E_g for traditional TiO_2 nanofilms is 3.26 eV), suggesting the reduction of the band gap due to the presence of localized energy levels and the increase of the conversion efficiency of solar energy. The enhanced visible regions can be attributed to the transfer of photo-generated electrons from Au to TiO_2, extending the light absorption of the Au/TiO_2 nanorods to larger wavelength due to the LSPR effect[27-29]. With the aim of determining the separation efficiency of photo-generated electrons and holes with two photoanodes, the on-off switches in the time slot of 0~180 s were measured by alternately illuminating and darkening, the devices at an interval of 30 s and 0 V, as shown in Fig.4b. In contrast to the traditional TiO_2 nanofilms, a sharp increase and no delay in photocurrent density suggest a fast start of cell operation at irradiation. No obvious reduction in photocurrent density in each "on" state indicates no apparent electron recombination kinetics. In addition, the values of the photocurrent reach plateau for the irradiation time more than 140 s. This result suggests that the Au in the Au/TiO_2 nanorods reduces the band-gap, improves the separation efficiency of photo-generated electrons and holes, and significantly increases the production of photocurrent. The suppression of charge recombination in Au/TiO_2 nanorods was confirmed by photoluminescence (PL) emission spectra. As known, the PL emission intensity can be used to evaluate the efficiency of the trapping, migration, and transfer of charge carriers in order to understand the fate of electron-hole pairs in semiconductor particles[30,31]. Fig.4c shows the PL

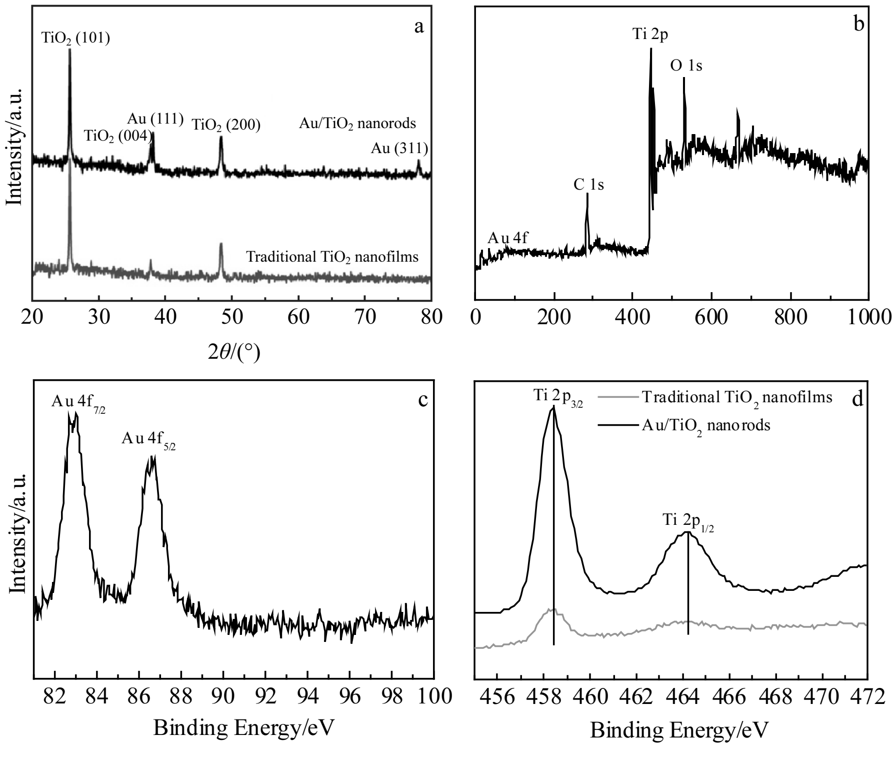

Fig.3 XRD patterns of the Au/TiO_2 nanorods (a) and XPS spectra of the Au/TiO_2 nanorods (b), Au 4f (c), and Ti 2p (d)

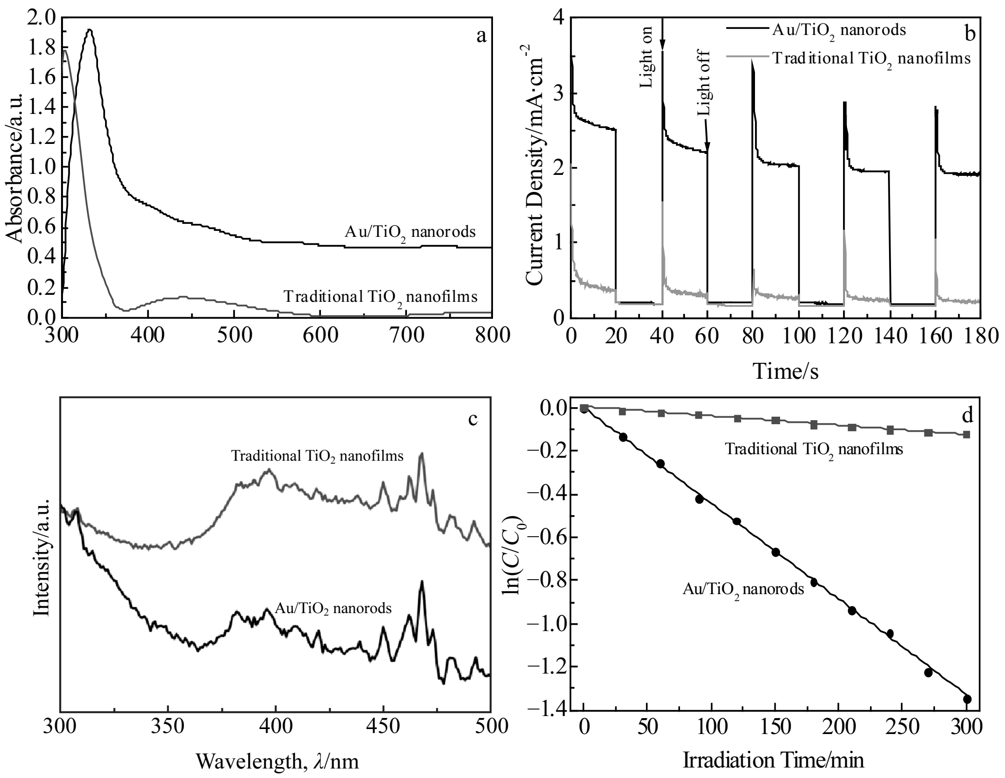

Fig.4 UV-vis diffuse reflection spectra (a), temporal evolution of photocurrent response (b), photoluminescence emission spectra (c), and temporal evolution of the concentration (d) of the MB organic compound in aqueous solution under the irradiation of visible light

intensity of both traditional TiO_2 nanofilms and Au/TiO_2 nanorods by magnetron sputtering. The emission intensity of Au/TiO_2 is much smaller than that of TiO_2 nanofilms in spite of the similar emissionpeaks. The lower PL intensity of Au/TiO_2 sample indicates a delay in recombination rate and, thus, higher photocatalytic activity. Fig.4d shows the temporal evolution of the normalized concentration of the MB organic compound in the aqueous solutions under the irradiation of visible light. For comparison, Au/TiO_2 nanorods have apparently improved the photo-degradation of the MB organic compound in the aqueous solution under the irradiation of visible light, which further demonstrates the formation by magnetron sputtering of Au/TiO_2 enhances the efficiency of photodegradation of MB.

3 Conclusions

1) Well-aligned Au/TiO_2 nanorods can be realized by a dc reactive magnetron sputtering strategy for catalysts applications. Compared with traditional TiO_2 nanofilms fabricated by the similar method, the Au/TiO_2 nanorods show high absorptionand intensive response to the visible light.

2) The virtues of fast on-off and multiple start stability motivate the potential applications of such aligned Au/TiO_2 nanorods in the degradation of MB.

3) The Au nanoparticles are embedded in the TiO_2 nanorods of anatase phase. The Au/TiO_2 nanorods exhibit lower PL emission intensity than the pure TiO_2 nanofilms prepared by similar approach, suggesting that Au nanoparticles reduces the recombination rate of photo-induced electrons and enhances the photocatalytic activity of the TiO_2 nanorods.

References

1 Wu H B, Hng H H, Lou X W. *Adv Mater*[J], 2012, 24(19): 2567
2 Gupta S M, Tripathi M. *Chin Sci Bull*[J], 2011, 56(17): 1639
3 Okubo N, Nakazawa T, Katano Y *et al. Applied Surface Science*[J], 2002, 197-198: 679
4 Ochiai T, Hoshi T, Slimen H *et al. Catal Sci Technol*[J], 2011, 1(8): 1324
5 Premchand Y D, Djenizian T, Vacandio F *et al. Electrochem Commun*[J], 2006, 8(12): 1840
6 Pang Y L, Lim S, Ong H C *et al. Appl Catal A-Gen*[J], 2014, 481: 127
7 Dawan F, Morampudi N, Jin Y *et al. Microelectron Eng*[J], 2014, 114: 105
8 Kumar S G, Devi L G. *J Phys Chem A*[J], 2011, 115(46): 13 211
9 Wang C H, Zhang X T, Shao C L *et al. J Colloid Interf Sci*[J], 2011, 363(1): 157
10 Luo Z X, Yang W S, Peng A D *et al. Nanotechnology*[J], 2009, 20(34): 2467
11 Park J T, Patel R, Jeon H *et al. J Mater Chem*[J], 2012, 22(13): 6131
12 Zhou X S, Yang F, Jin B *et al. Mater Lett*[J], 2013, 112: 145

13 Zhong P, Que W X, Zhang J. *J Nanosci Nanotechno*[J], 2010, 10(11): 7574

14 Yoon S B, Woo B C, Chung S J *et al. J Nanosci Nanotechno*[J], 2012, 12(2): 1604

15 Sulka G D, Kapusta-Kolodziej J, Brzozka A *et al. Electrochim Acta*[J], 2010, 55(14): 4359

16 Ren X, Gershon T, Iza D C *et al. Nanotechnology*[J], 2009, 20(36): 365604

17 Kawazu M, Nara M, Tsujino T. *J Sol-Gel Sci Techn*[J], 2004, 31(1-3): 109

18 Macwan D P, Dave P N, Chaturvedi S. *J Mater Sci*[J], 2011, 46(11): 3669

19 Yu H, Pan J, Bai Y *et al*. *Chem-Eur J*[J], 2013, 19(40): 13 569

20 Lai T M, Yi L, Yang W X. *Chem Lett*[J], 2010, 39(3): 294

21 Du J M, Zhang J S, Kang D J. *Crystengcomm*[J], 2011, 13(12): 4270

22 Feng C Q, Tang J, Zhang C F *et al. Nanosci Nanotech Lett*[J], 2012, 4(4): 430

23 Acayanka E, Djowe A T, Laminsi S *et al. Plasma Chem Plasma P*[J], 2013, 33(4): 725

24 Fang F, Kennedy J, Manikandan E *et al. Chem Phys Lett*[J], 2012, 521: 86

25 Li R Z, Zhou A H, Lu Q *et al. Colloids and Surfaces A-Physicochemical and Engineering Aspects*[J], 2013, 436: 270

26 Chang J H, Ellis A V, Hsieh Y H *et al. Sci Total Environ*[J], 2009, 407(22): 5914

27 Li Y K, Yu H M, Zhang C K *et al. Int J Hydrogen Energ*[J], 2013, 38(29): 13023

28 Subramanian V, Wolf E, Kamat P V. *J Phys Chem B*[J], 2001, 105(46): 11 439

29 Xie Y R, Wei L, Li Q H *et al. Nanoscale*[J], 2014, 6(15), 9116

30 Kao L C, Lin C J, Dong C L *et al. Chem Commun*[J], 2015, 51(29): 6361

31 Meng L J, Li C, Santos M P. *J Inorg Organomet P*[J], 2011, 21(4): 770

磁控溅射制备的 Au-TiO$_2$ 纳米棒阵列的光降解研究

孔少奇 [1,2]，宋选民 [1,2]，孙泽东 [1,2]，张纯旺 [1,2]，严国超 [1,2]

(1. 太原理工大学 矿业工程学院，山西 太原 030024)

(2. 太原理工大学 采矿工艺研究所，山西 太原 030024)

摘　要：通过磁控溅射制备了对齐的 Au-TiO$_2$ 纳米棒阵列，Au-TiO$_2$ 纳米棒的制备通过直流反应磁控溅射法在室温中进行，之后在 500 ℃的空气中热处理 2 h，热处理导致 Au-TiO$_2$ 纳米棒的 Au 纳米粒子嵌入到锐钛矿相 TiO$_2$ 纳米棒中，与传统方法制备的纯 TiO$_2$ 纳米棒相比，这些 Au-TiO$_2$ 纳米棒表现出较低的光致发光强度和较高的光吸收性，并且对可见光反应强烈。TiO$_2$ 纳米棒中的 Au 纳米颗粒能够抑制电荷复合。

关键词：Au-TiO$_2$ 纳米棒；光降解；磁控溅射；光致发光强度

作者简介：孔少奇，男，1989 年生，博士，太原理工大学采矿工艺研究所，山西 太原 030024，电话：0351-6014627，E-mail: tjdxksq@sina.com